strain
An International Journal for Experimental Mechanics

Damage Characterisation of Inhomogeneous Materials: Experiments and Numerical Simulations of Wave Propagation

D. G. Aggelis

Department of Materials Science and Engineering, University of Ioannina, 45110 Ioannina, Greece

ABSTRACT: Elastic waves are commonly used for characterisation of concrete. To produce reliable results, wave propagation needs a lot of understanding. Therefore, combined study through experiments and simulations is deemed essential. In the present paper, the case of concrete with flakey inclusions, serving as micro-cracks, is investigated both in laboratory experiments and computer simulation. The results suggest new wave features suitable for characterisation. Parameters like wave dispersion and frequency dependent attenuation prove to be more sensitive to damage than the traditionally used pulse velocity and can improve characterisation when employed *in situ*. The monitoring of a cracked concrete bridge before and after repair is discussed as a case study.

KEY WORDS: *attenuation, concrete, damage, dispersion, inhomogeneity, simulation*

Introduction

Evaluation of concrete quality is a subject-concentrating effort of the engineering community for many decades. This is because the catastrophic failure or malfunction of civil infrastructure can lead to human casualties as well as high financial cost. Concerning specific macroscopic flaws, like bridge cracks, delaminations or ungrouted tendon ducts, accurate characterisation is possible [1–3]. For distributed damage though, the traditionally used pulse velocity can provide only rough estimations [4–6]. Despite its reduced sensitivity, pulse velocity has certain advantages. One is that it exhibits limited dependence on the length of propagation path, the type of transducers as well as the coupling conditions. Another is that it can be measured using very simple equipment, without the need of delicate waveform analysis, and therefore, it has been used for more than 50 years. This leads to the next advantage which is the long-established, although rough, correlations with concrete strength [7–10]. Nowadays, waveform acquisition is standard to most of the available equipment for ultrasonic testing. Therefore, the additional use of other simple features that draw information from the whole pulse is not hindered.

The present paper aims to indicate some features that take advantage of the scattering parameters of the material, to characterise more accurately the material condition. Experimental measurements were conducted in cementitious material containing small light inclusions to simulate distributed damage in different volume contents. It is seen that the inclusions influence pulse velocity but they have stronger influence on other parameters like velocity dispersion (frequency dependence) as well as high attenuation for high frequencies [10, 11] because of extensive scattering. As wave propagation in material with damage is an extremely complicated subject, numerical simulations are used to shed light and understand the contribution of different parameters (frequency, orientation of cracks) on the finally measured wave features. In this way, new features can be suggested and applied in actual practice when possible, as will be shown in a case study obtained from a bridge ultrasonic monitoring.

Materials

The materials were cubic mortar specimens of 150 mm side. The mortar matrix had a water to cement ratio by mass, w/c of 0.5 and sand to cement, s/c of 3. The maximum size of sand grain was 3 mm. The inclusions were cut from commercially available vinyl sheets of different thicknesses. The case presented in this paper concerns inclusions with shape of $15 \times 15 \times 0.5$ mm. The plate shape resembles actual cracks much closer than the spherical shape that has been used in other research works. The inclusions were added to each specimen at different volumes after the other mortar ingredients had

doi: 10.1111/j.1475-1305.2009.00721.x

already been mixed. Therefore, mortar specimens with namely 0, 1, 5 and 10% by volume of vinyl inclusions were produced. Details about the mixture preparation can be found in [10]. It is mentioned that cracks in actual material contain most likely air. However, it would not be possible to have realistic crack shapes by air entrainment in the samples. Using vinyl sheet, it was easy to adjust the thickness of the 'cracks' and obtain the film shape which resembles much better the actual crack size than the spherical air voids. In any case, the acoustic impedance of vinyl is almost negligible compared with the concrete matrix (approximately 1/8), which is certain to result in strong scattering effects.

Stress Wave Measurements

Wave measurements were conducted in through-the-thickness, as well as surface mode. The setup is a simple ultrasonic configuration utilising one pulser and one receiver for through transmission (wavepath of 150 mm). For the phase velocity measurements, where a broad band excitation was needed, the PAC C-101-HV pulse generator was used. Combined with the broadband sensors (FC 1045S, Fuji ceramics Corporation, Tokyo, Japan), a relatively wide band from 0 to 500 kHz was examined. A layer of silicone grease was applied to ensure acoustical coupling while the received signal was pre-amplified, digitised with a sampling rate of 10 MHz (sampling time 0.1 μs) and stored in an acoustic emission acquisition system (Mistras 2001; Physical Acoustics Corporation, Princeton, NJ, USA), PAC. Considering that the transit time through 150 mm of mortar is more than 35 μs, this sampling rate employs an error of about 0.3%.

Phase Velocity Measurements

To derive the dispersion curve (or the velocity of each frequency component), monochromatic pulses should be excited. This is not always possible and additionally, a large number of pulses of different frequencies should be used to draw in detail the dispersion curve. The dispersion curve can be calculated alternatively by using a wide band excitation and sensors in a fashion similar to Sachse and Pao [12]. This way, the velocity of each frequency component can be calculated for the range that is clearly transmitted by one broad band pulse. Using fast Fourier transformation (FFT), the 'phase' of the excited and the received wave is calculated and unwrapped. The difference between the phase of the excited and received pulses is calculated for each frequency component of the Fourier spectrum and it leads to the calculation of the phase velocity for that frequency. The description of the whole procedure is beyond the scope of this manuscript. The interested reader can be directed to the original paper of Sachse and Pao [12]. It is mentioned that only the first two cycles of the waveforms are used while the rest is zero-padded. This is to avoid any reflection or other types of waves arriving later than the longitudinal, as well as the possible ringing behaviour of the sensor.

The phase velocity curves calculated for different materials of this study are depicted in Figure 1. Additionally, the phase velocity of a cement paste specimen is depicted in the same figure. It is seen that the dispersion curve of paste is horizontal, exhibiting no variation of velocity with frequency. This can be easily attributed to homogeneity because the material does not contain any inclusions or sand. However, plain mortar exhibits a slight variation, with the velocity of bands near 500 kHz measured at a value about 3% higher than 10 kHz. Similar trend is observed for mortar with 1% inclusions. Further addition of light inclusions lowers the curve and enhances the dispersion, making the increase of velocity with frequency more obvious. For the case of 5% inclusions, the increase of velocity is 8.5% and for the 10% case the increase is even higher, at 21.5%. This trend of inclusion-rich mortar is a certain manifestation of dispersion due to inhomogeneity that can be expected in actually damaged material.

This behaviour is typical for multiphase materials when scattering is the dominant propagation mechanism. It has been measured that the phase velocity of a composite medium may exhibit variations relatively to the matrix velocity at low frequencies for composites of solids in solids, solids in liquid

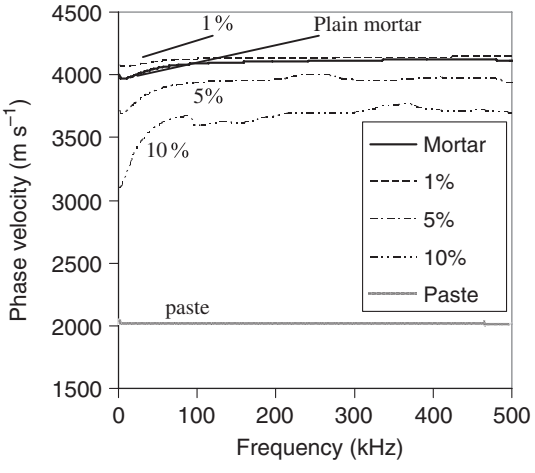

Figure 1: Phase velocity versus frequency curve for mortar with various inclusion contents

doi: 10.1111/j.1475-1305.2009.00721.x

suspensions or even bubbles in fresh cement paste [13–16]. However, for the higher frequencies tested, the phase velocity of the composite converges to a value closer to the velocity of the matrix.

As to concrete, similar dispersion studies are limited. However, for the simple case of spherical light inclusions [11] the trend has been found similar with the present results; the phase velocity of 'damaged' mortar at 1 MHz was approximately 500 m s^{-1} higher than the velocity of 200 kHz. The above show that not only pulse velocity but also the dependence of velocity on frequency can supply information on the inhomogeneity condition of concrete.

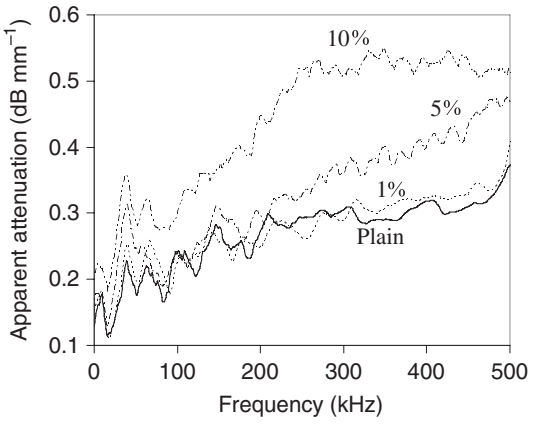

Figure 2: Attenuation versus frequency curve for mortar with different content of inclusions

Attenuation Behaviour

Stress wave transmission in concrete has been related to the aggregate content and size [17], however, without establishment of a certain correlation between inclusion size and attenuation [18–21]. Air bubbles (entrapped or intentionally entrained) seem also to influence the behaviour in hardened [19, 22] or fresh cementitious material [16]. Distributed damage evolved by subjection of concrete to freezing–thawing cycles has also been proven to increase attenuation [11, 23].

In the present case, the overall material attenuation coefficient, $\alpha(f)$, was calculated using the frequency response of the specimen in through transmission mode, A(f) and the reference spectrum B(f):

$$\alpha(f) = -(20/x) \times \log[A(f)/B(f)] \quad (1)$$

where x is the propagation distance (150 mm), f is the frequency and B(f) is the spectrum of the sensors' face to face response. As the reference signal is the face to face response of the sensors and not a pulse at a certain point of the material, the term 'apparent attenuation' is used. This is necessary because the transmitted pulse can be measured only at one point, i.e. the surface where the receiver is placed. In any case, any comparison of different materials is valid because the reference signal is constant; therefore, any change in attenuation is attributed to the material itself. The wide-band sensors were used to provide information for a broad frequency band. The face-to-face response can be considered close to the pulse entering the material. The difference of amplitudes of the sent and received signals, although cannot provide an absolute measure of material attenuation, gives an indication of the signal transmission through the thickness of concrete and has been used for evaluation of concrete deterioration after freezing–thawing cycles, as well as characterisation of the aggregate content [17, 23].

In Figure 2, the attenuation coefficient of mortar with different inclusion content is depicted. It increases for all materials up to 500 kHz. Material with 10% of inclusions exhibits constantly the highest attenuation with larger difference above 100 kHz. The case of 5% of inclusions is the second most attenuative for most frequencies. Finally, although seemingly very close, the 1% case is constantly more attenuative than the plain mortar for the band 0–100 kHz, as well as above 300 kHz. It is seen therefore, that as has been suggested [23, 24] energy parameters are more sensitive to damage than velocity. In this experimental series, the velocity of mortar with 10% inclusions is approximately 20% lower than the plain mortar's one, as seen in Figure 1. However, attenuation increases by almost 50% for the low frequencies around 50 kHz and is almost double for frequencies more than 200 kHz.

It seems that the potential for characterisation increases with frequency. However, the attenuation is large enough to constitute examination with high frequencies impossible in most full-scale, damaged concrete structures. Still, the study of transmission features other than pulse velocity even at low frequencies can certainly enhance the characterisation.

Surface Wave Propagation

Similar measurements have been conducted for measurement of Rayleigh waves on the surface of the specimens. Rayleigh waves contain higher amount of energy and therefore, are more suitable for cases of damage characterisation on or near the surface of structures. The experimental setup consists of three wide band piezoelectric transducers with high

doi: 10.1111/j.1475-1305.2009.00721.x

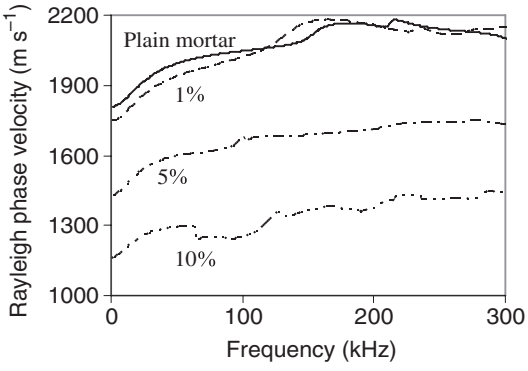

Figure 3: Rayleigh dispersion curve of concrete with different inclusion contents

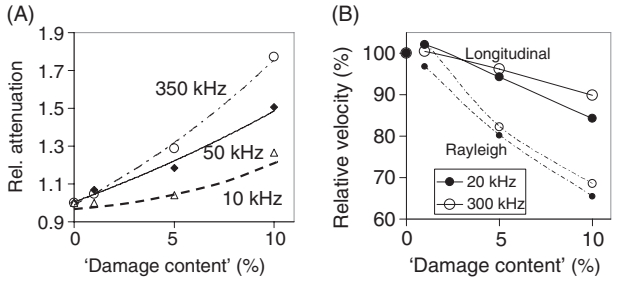

Figure 4: (A) Attenuation and (B) wave velocity versus damage content for various frequencies

sensitivity up to 1 MHz. They were placed on the same surface of the specimen (cube of 150 mm side), in a straight line, with a centre to centre distance of 20 mm. The excitation was conducted 20 mm away from the first receiver by pencil lead break, which introduces frequencies up to 300 kHz. The coupling between the sensors and the mortar surface was enhanced by roller bearing grease and no pressure was applied on the sensors to minimise any influence on the propagating wave [25].

Rayleigh phase velocity

As the medium is strongly inhomogeneous, each frequency component could be influenced in a different way, imposed by the content and size of the scatterers. The pulse used (pencil lead break), contains energy up to 300 kHz and it is interesting to examine how each frequency component behaves. Therefore, the frequency-dependent phase velocity of the Rayleigh is calculated. The Rayleigh contribution is masked by the faster types (longitudinal and shear waves). However, the energy of the Rayleigh waves is much higher than the other contributions and therefore, isolating a part of the signal where the Rayleigh is expected, can yield information about this wave type with very little influence from other types. In this case, a window of 30 μs around the major Rayleigh arrivals was isolated and the rest of the waveform was zero-padded [26]. Using FFT, the phase of the waveform was calculated and unwrapped. Therefore, the phase difference between waveforms collected at different distances from the excitation (i.e. the first and third receiver with a propagation distance of 40 mm) leads to the calculation of phase velocity versus frequency curve as also explained earlier [12]. The results are depicted in Figure 3 for materials with different inclusion contents.

It is seen that plain mortar exhibits dispersive behaviour, with velocity increasing up to about 200 kHz. The increased inhomogeneity induced by the plastic inclusions influences the velocity behaviour more strongly. Material with 10% inclusions exhibits the lowest curve, but even 1% of vinyl changes the curve compared with plain mortar. At lower frequencies, the curves exhibit high gradients. However, above 100 kHz the changes are not as abrupt. This is a trend mentioned in many different multi-phase systems. Composites of solids in solids, or suspensions of solids in liquids exhibit similar trends [27], with the velocity converging at higher frequencies to a value closer to the velocity of the matrix material.

As examined above, increasing the inhomogeneity of the medium, results in higher attenuation and lower velocities. The effect of frequency can be again seen in Figure 4A and B. Figure 4A shows that the attenuation increases much more for high frequencies (e.g. 350 kHz compared with 50 and 10 kHz). In this case, the attenuation of the different materials at specific frequencies (as displayed in Figure 2) is divided to the corresponding attenuation of plain mortar. This is of primary importance for *in situ* monitoring because so far the frequencies applied are usually 50 kHz. It is suggested that application of higher frequencies, whenever possible could yield clearer results because at these frequencies the attenuation is more sensitive to damage.

On the other hand, it is worth noting that the Rayleigh waves suffer greater decrease in velocity (more than 30%) than longitudinal (about 10%) (see Figure 4B). In this case also, the velocities of the different materials have been reduced to the velocity of plain mortar for the corresponding frequency. Therefore, it is preferable to rely on Rayleigh waves when a surface layer is to be examined as they appear more sensitive to damage.

Numerical Simulation

Numerical simulations enhance our understanding on wave propagation, highlighting the parameters that influence wave behaviour the most.

doi: 10.1111/j.1475-1305.2009.00721.x

Additionally, using simulations, a variety of different cases can be examined which are difficult or costly to examine experimentally. The velocity dispersion exhibited by the concrete with realistic cracks, as described above, is a phenomenon that deserves numerical investigation because scattering theory produces results for spheroid inclusions only.

The simulations were conducted with commercially available software [28]. The fundamental equation governing the two-dimensional propagation of stress waves in a perfectly elastic medium, ignoring viscous losses is seen below:

$$\rho \frac{\partial^2 u}{\partial t^2} = \mu \nabla^2 u + (\lambda + \mu) \nabla \nabla u \quad (2)$$

where $u = u(x,y,t)$ is the time-varying displacement vector, ρ is the mass density, λ and μ are the first and second Lame constants respectively, while t is the time. The focus, from the engineering point of view is given on simulating the actual cases examined experimentally. However, certain pre-requisites should be followed for the analysis to lead to reliable results concerning mainly the time and space resolution, as will be mentioned later. The software used operates by solving the above equation based on a method of finite differences. Equation (2) is solved with respect to the boundary conditions of the object, which include the input source that has pre-defined time-dependent displacements at a given location and a set of initial conditions [28]. For heterogeneous media like the one studied herein, propagation in each distinct homogeneous phase (in this case mortar matrix and inclusions) is solved according to Equation (2), while the continuity conditions for stresses and strains must be satisfied on the interfaces [28].

In this case, all materials were considered elastic with no viscosity components. Materials and geometry were set similar to the experiment. The material properties used for mortar are: elasticity modulus $E = 36$ GPa, Poisson's ratio, $\nu = 0.2$ and density $\rho_m = 2300$ kg m^{-3}, while for the vinyl inclusions $E = 3$ GPa, $\nu = 0.3$ and $\rho_i = 1200$ kg m^{-3}. The specimen geometry is a square of 150-mm side and displacement excitation is introduced on one side. The simulated transducer and receiver are 15-mm long to resemble the actual transducers used in the experiment [10] and are placed on opposite sides of the geometry, i.e. the propagation distance is 150 mm (see Figure 5). The receiver computes the average lateral displacement on its defined length.

The possible combinations of shapes, sizes, orientations and concentrations of inclusions are limitless. The simulations presented herein were performed using the inclusions shape similar to the cross-section of the experimentally used one, specifically 15×0.5 mm, neglecting the third dimension of 15 mm of the actual inclusions to reduce the problem to two dimensions [29]. The thickness was typical of large crack openings in concrete. The other dimensions were indicatively chosen just to be much larger than the thickness and produce the thin plate shape. Some extreme cases of orientation were tested, namely parallel and vertical to the propagation, as seen in Figure 5A and B. The case of 45° orientation was also examined, as well as the classic case of spherical inclusions. It should be mentioned that whichever pattern was selected still it would just be one case of the infinite number of possible cases. Therefore, some marginal cases were selected in this study, including the horizontal which is the most 'favourable' for wave propagation because it does not cause strong reflection to the wavefront and the vertical which causes reflections each time the wave hits on an inclusion. After some trials, the spacing resolution for the calculation was set to 0.2 mm (0.008 in.) while 0.1 mm resolution tried in indicative cases resulted in exactly the same waveforms but was much more time consuming. The wavelength even for the highest simulated frequency of 150 kHz was approximately 25 mm two orders of magnitude

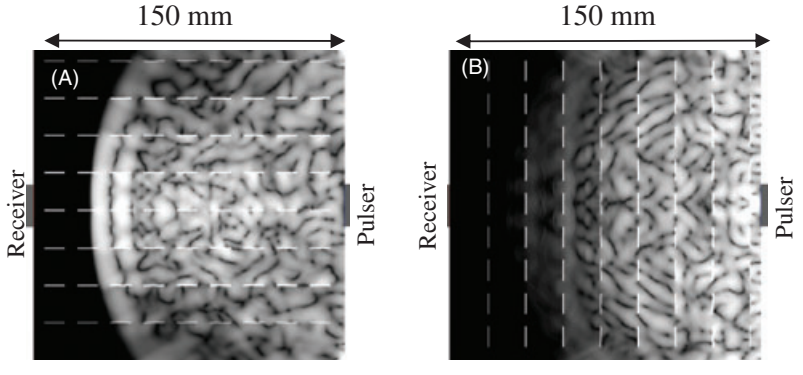

Figure 5: Displacement field inside mortar with (A) horizontal cracks, (B) vertical cracks. The inclusions are 15×0.5 mm

doi: 10.1111/j.1475-1305.2009.00721.x

longer than the spacing resolution. The resolution in time was 0.16124 μs. The frequencies applied (from 10 to 150 kHz) resulted in cycle duration of 6.67 to 100 μs. Therefore, a cycle included at least 40 points ensuring accurate depiction.

Numerical results

In Figure 5, besides the arrangement of the inclusions, one can see the displacement field, approximately 30 μs after the excitation. Both cases of Figure 5 concern inclusion content of 1% by cross-section area. It can be confirmed by visual observation of the displacement field, that the case of inclusions vertical to the propagation (Figure 5B) causes the strongest distortion of the wavefront. This is reasonable because a significant part of the energy is reflected back at each encounter by the large surface of the perpendicular inclusions. The parallel case (Figure 5A) does not influence much the forward direction.

In Figure 6A, velocities measured from the onset of simulated waveforms with respect to the horizontal arrangement of the thin inclusions and different volume contents are depicted. The velocity tends to increase with frequency. The perpendicular orientation (Figure 6B) results in much lower velocities, even less than 3000 m s^{-1} for 10% of damage.

The above numerical results support the experimental dispersive trends. The velocity of a homogeneous matrix is constant while as the inhomogeneity increases the velocity becomes more dependent on the frequency. This dependence is quite strong (5% change corresponds to 200 m s^{-1}, as seen in Figure 6) and can be captured by a simple ultrasonic setup. Thus, it provides and additional parameter for characterisation to assist the long established correlations of pulse velocity with strength and structural condition. It is reminded that the simulation results were produced neglecting the viscous character of the materials. As the results come close to the experimental it is suggested that elastic scattering is the dominant mechanism for the dispersion.

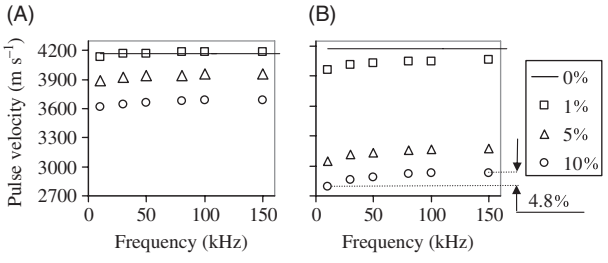

Figure 6: Numerical results of pulse velocity for different frequency and inclusion contents, (A) horizontal orientation, (B) vertical

It can be concluded that, as the inhomogeneity increases, the velocity decreases and the dispersion increases. This is reasonable because inhomogeneity is the source of dispersion and therefore, increase in its content results in more highlighted dispersive effects. The significance is that the use of different frequencies will enhance the discrimination between homogeneous and inhomogeneous material because the dispersion (or the increase of velocity) throughout the low frequency band up to 150 kHz, seems very sensitive to the existence of damage. Practically, to examine the dispersion of concrete, velocity measurements should be done at low frequencies (suggested 10 kHz) and higher (150 kHz). In case, the velocity difference between the two frequencies is high (around 200 m s^{-1} or more) this will imply strong inhomogeneity, while if the velocities at 10 and 150 kHz are similar (within 50 m s^{-1}) this implies sound material. As an example of dispersion examination, a case of through the thickness crack characterisation in a concrete bridge follows.

Example of Crack Characterisation Using Wave Dispersion

This section describes a case of field monitoring where dispersion features enhanced the results of ultrasonic measurements. It concerns a concrete bridge that developed through the thickness cracks on the lower deck [3]. The cause is supposed to be the combined effect of shrinkage and premature removal of the mechanical support, which led to overloading before adequate hardening of the material. Therefore, the inspection was conducted using ultrasound before, as well as after injection of epoxy to characterise the repair effectiveness. The objective of this repair method is to fill the crack and bond the concrete on both sides of the crack. Ultrasonic wave measurement and analysis were conducted for all cracks, whereas in this paper an indicative case will be described. The crack width at the surface was 0.2 mm.

The experimental arrangement can be seen in Figure 7. Totally 10 sensors were used; five on each surface in a way that the crack was between the 8th and 9th on the upper side, while the array was parallel to the axis of the structure. The sensors used exhibit high sensitivity at bands below 150 kHz. The data acquisition system was an acoustic emission monitoring multi-channel system, while the sampling rate was set to 10 MHz. The excitation was conducted by pencil lead break. Excitation was applied at each sensor position consecutively. The waveforms received from the opposite side are used

doi: 10.1111/j.1475-1305.2009.00721.x

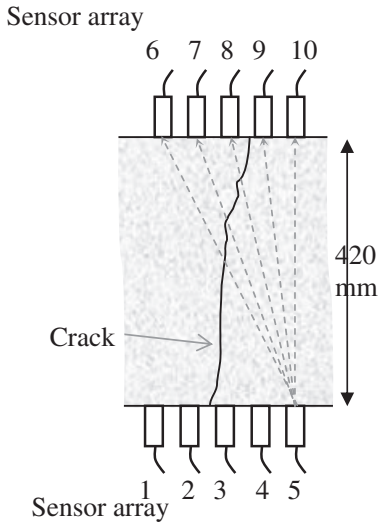

Figure 7: Side view of the concrete deck and the sensors' arrays

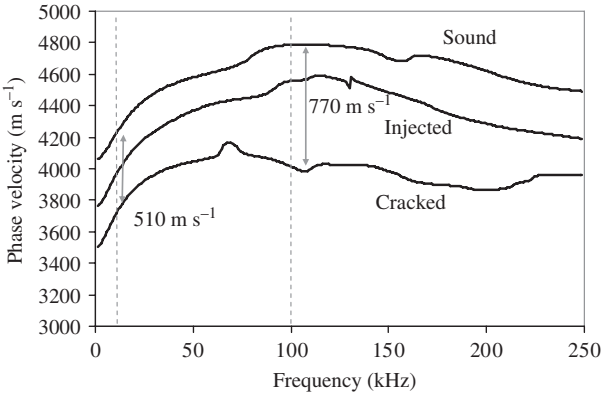

Figure 8: Dispersion curves for concrete at different states

for calculation of phase velocity curves of the concrete. In this case, the first peak is isolated, similarly to [17] and the same procedure with FFT and phase difference calculation is conducted. Examples of longitudinal wave phase velocities are depicted in Figure 8. The velocity of healthy material increases with frequency up to 100 kHz, while the cracked path results in much lower curve. Low frequencies around 10 kHz exhibit phase velocity of 3600 m s^{-1}, 510 m s^{-1} lower than the intact state. Correspondingly, frequencies at the vicinity of 100 kHz, present even greater discrepancy of almost 800 m s^{-1} (4000 for cracked and 4800 m s^{-1} for intact). The repaired material is in any case in between. As the velocity differences between the cracked, the repaired and the sound situation are not the same for each frequency component but seem to be highlighted for frequencies around 100 kHz, it was assumed reasonable to conduct the tomography procedure using velocities of different frequencies. Therefore, for all different wave paths (total number 50) between each impact point and receiver, the corresponding dispersion curve was calculated. Then for any selected frequency the corresponding phase velocity of all the wave paths was picked and fed to the tomography software [30]. Herein, two indicative cases are discussed corresponding to lower and higher frequency bands acquired, namely 10 and 100 kHz as seen in Figure 9. In Figure 9A and B, one can observe the tomogram of the region of interest before and after the impregnation for the frequency of 10 kHz, while Figure 9C and D concerns the case of 100 kHz. For both frequencies, the repair effect is obvious, elevating the average velocity of the cells by 300 m s^{-1} for the case of 10 kHz and by about 450 m s^{-1} for 100 kHz. The areas showing the defect are substantially eliminated in both cases. However, the tomogram of 100 kHz seems more accurate concerning the location of the defect, because as mentioned above, the crack in this case was not exactly vertical, but slightly inclined. Also, as the colour variation implies, the difference of

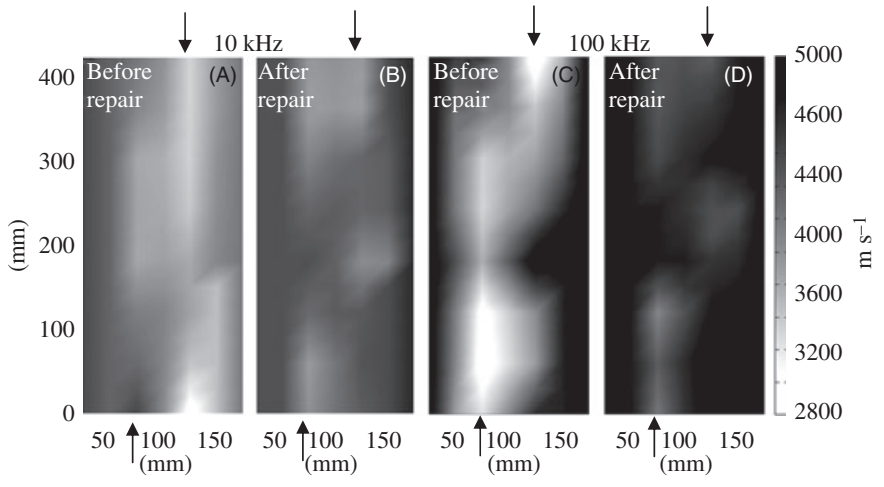

Figure 9: Tomograms of the bridge deck cross-section at (A) 10 kHz before, (B) after repair, (C) 100 kHz before and (D) after repair. The arrows show the crack opening points

doi: 10.1111/j.1475-1305.2009.00721.x

maximum to minimum (healthy to cracked) for Figure 9A is 31%, while for Figure 9C the difference is 49%. This shows that, propagation at higher frequencies is more sensitive to the damage than lower frequencies in this case. The interaction between inhomogeneity parameters, such as size and content, and stress wave velocity is not always easy to understand. However, in the specific case of this continuous through-the-thickness defect, the velocity of higher frequencies is more sensitive and therefore, appropriate for assessment of the repair effect.

It should be mentioned that the accurate characterisation of the degree of filling of the crack volume with epoxy is not possible. However, the tomography analysis revealed that at least a substantial portion was impregnated, because the propagation in terms of velocity was mainly restored. Furthermore, using the velocity at different frequencies, one can compare which information is more accurate. It is seen that higher frequencies in this case produced better results. In the specific case, this was done using the same equipment and shows that without additional cost or time, the information may be improved by taking advantage of wave dispersion. So far the results are based on the pulse velocity which is measured by the first arrival of the wave. However, making use of the phase velocity at different frequencies can produce more accurate results concerning damage and repair characterisation.

Conclusions

In the present paper, stress wave propagation in concrete is studied through experiments and simulations. It is concluded that concrete exhibits wave dispersion which is revealed by velocity dependence on frequency. The dispersion depends on the damage content. It is suggested therefore, that velocity measurements can be conducted with a low and a high frequency (e.g. 10 and 150 kHz). In case, the difference in velocity is below 50 m s^{-1}, homogeneous material is implied, while dispersion of more than 200 m s^{-1} shows strong inhomogeneity. The specific values mentioned concern the case of laboratory specimens of this study examined by longitudinal waves. In case of an actual structure with different internal condition (e.g. heavy metal reinforcement), the dispersion trends could change, but examination of wide band of frequencies enhances the characterisation in any case. The examination at different frequencies is demonstrated in a case study of concrete bridge deck, where the tomogram of a through-the-thickness crack is more accurate at 100 kHz than 10 kHz.

REFERENCES

1. Malhotra, V. M. and Carino, N. J. (eds) (1991) *CRC Handbook on Nondestructive Testing of Concrete*. CRC Press, Florida.
2. Ohtsu, M. and Watanabe, T. (2002) Stack imaging of spectral amplitudes based on impact-echo for flaw detection. *NDT&E Int.* **35**, 189–196.
3. Aggelis, D. G. and Shiotani, T. (2007) Repair evaluation of concrete cracks using surface and through-transmission wave measurements. *Cement Concrete Compos.* **29**, 700–711.
4. Popovics, S. (2001) Analysis of the Concrete Strength versus Ultrasonic Pulse Velocity Relationship. *Mater. Eval.* **59**, 123–130.
5. Popovics, S. and Popovics, J. S. (1991) Effect of stresses on the ultrasonic pulse velocity in concrete. *Mater. Struct.* **24**, 15–23.
6. Van Hauwaert, A., Thimus, J. F. and Delannay, F. (1998) Use of ultrasonics to follow crack growth. *Ultrasonics* **36**, 209–217.
7. Kaplan, M. F. (1959) The effects of age and water/cement ratio upon the relation between ultrasonic pulse velocity and compressive strength. *Mag. Con. Res.* **11**, 85–92.
8. Jones, R. (1953) Testing of concrete by ultrasonic-pulse technique. *Proceedings of the thirty-second annual meeting. Highway Research Board* **32**, 258–275.
9. Anderson, D. A. and Seals, R. K. (1981) Pulse velocity as a predictor of 28- and 90-day strength. *ACI J.* **78-9**, 116–122.
10. Shiotani, T. and Aggelis, D. G. (2009) *Wave propagation in concrete containing artificial distributed damage. Mater. Struct.* **42**, 377–384.
11. Chaix, J. F., Garnier, V. and Corneloup, G. (2006) Ultrasonic wave propagation in heterogeneous solid media: theoretical analysis and experimental validation. *Ultrasonics* **44**, 200–210.
12. Sachse, W. and Pao, Y.-H. (1978) On the determination of phase and group velocities of dispersive waves in solids. *J. Appl. Phys.* **49**, 4320–4327.
13. Kinra, V. K. and Rousseau, C. (1987) Acoustical and optical branches of wave propagation. *J. Wave Mater. Interact.* **2**, 141–152.
14. Mobley, J., Waters, K. R., Hall, C. H., Marsh, J. N., Hughes, M. S., Brandenburger, G. H. and Miller, J. G. (1999) Measurements and predictions of phase velocity and attenuation coefficient in suspensions of elastic microspheres. *J. Acoust. Soc. Am.* **106**, 652–659.
15. Cowan, M. L., Beaty, K., Page, J. H., Zhengyou, L. and Sheng, P. (1998) Group velocity of acoustic waves in strongly scattering media: dependence on the volume fraction of scatterers. *Phys. Rev. E.* **58**, 6626–6636.
16. Aggelis, D. G., Polyzos, D. and Philippidis, T. P. (2005) Wave dispersion and attenuation in fresh mortar: theoretical predictions vs. experimental results. *J. Mech. Phys. Solids* **53**, 857–883.
17. Philippidis, T. P. and Aggelis, D. G. (2005) Experimental study of wave dispersion and attenuation in concrete. *Ultrasonics* **43**, 584–595.
18. Landis, E. N. and Shah, S. P. (1995) Frequency-dependent stress wave attenuation in cement-based materials. *J. Eng. Mech.-ASCE* **121**, 737–743.

doi: 10.1111/j.1475-1305.2009.00721.x

19. Kim, Y. H., Lee, S. and Kim, H. C. (1991) Attenuation and dispersion of elastic waves in multi-phase materials. *J. Phys. D Appl. Phys.* **24**, 1722–1728.
20. Gaydecki, P. A., Burdekin, F. M., Damaj, W., John, D. G. and Payne, P. A. (1992) The propagation and attenuation of medium-frequency ultrasonic waves in concrete: a signal analytical approach. *Meas. Sci. Technol.* **3**, 126–134.
21. Jacobs, L. J. and Owino, J. O. (2000) Effect of aggregate size on attenuation of Rayleigh surface waves in cement based materials. *J. Eng. Mech.-ASCE* **126**, 1124–1130.
22. Punurai, W., Jarzynski, J., Qu, J., Kurtis, K. E. and Jacobs, L. J. (2006) Characterization of entrained air voids in cement paste with scattered ultrasound. *NDT&E Int.* **39**, 514–524.
23. Shah, S. P., Popovics, J. S., Subramanian, K. V. and Aldea, C. M. (2000) New directions in concrete health monitoring technology. *J. Eng. Mech.-ASCE* **126**, 754–760.
24. Selleck, S. F., Landis, E. N., Peterson, M. L., Shah, S. P. and Achenbach, J. D. (1998) Ultrasonic investigation of concrete with distributed damage. *ACI Mater. J.* **95**, 27–36.
25. Aggelis, D. G. and Shiotani, T. (2007) Surface wave propagation in strongly heterogeneous media, J. *Acoust. Soc. Am.* **122**, EL151–EL157.
26. Dokun, O. D., Jacobs, L. J. and Haj-Ali, R. M. (2000) Ultrasonic monitoring of material degradation in FRP composites. *J. Eng. Mech.* **126**, 704–710.
27. Aggelis, D. G., Tsinopoulos, S. V. and Polyzos, D. (2004) An iterative effective medium approximation (IEMA) for wave dispersion and attenuation predictions in particulate composites, suspensions and emulsions. *J. Acoust. Soc. Am.* **116**, 3443–3452.
28. Luo, G., Kaufman, J. J., Chiabrera, A., Bianco, B., Kinney, J. H., Haupt, D., Ryaby, J. and Siffert, R. S. (1999) Computational methods for ultrasonic bone assessment. *Ultrasound Med. Biol.* **25**, 823–830.
29. Aggelis, D. G. and Momoki, S. (2009) Numerical simulation of wave propagation in mortar with inhomogeneities. *Am. Concrete Inst. Mater. J.* **106**, 59–63.
30. Kobayashi, Y., Shiotani, T., Aggelis, D. G. and Shiojiri, H. (2007) Three-dimensional seismic tomography for existing concrete structures. *Proc. Second International Operational Modal Analysis Conference*, IOMAC 2007, April 30–May 2, Copenhagen, Vol. 2 595–600.

doi: 10.1111/j.1475-1305.2009.00721.x